Novel underlying genetic markers for asthenozoospermia due to abnormal spermatogenesis and reproductive organ inflammation

YAODONG ZHANG[1,2], YUN PENG[1], YAO WANG[1], JIAN XU[1] and HONGLI YAN[1]

[1]Reproductive Medicine Center, The First Affiliated Hospital of Naval Medical University, Shanghai 200433; [2]Department of Clinical Laboratory, The 971st Hospital of Chinese People's Liberation Army, Qindao, Shandong 266071, P.R. China

Received October 3, 2023; Accepted January 24, 2024

DOI: 10.3892/etm.2024.12434

Abstract. Asthenozoospermia, a male fertility disorder, has a complex and multifactorial etiology. Moreover, the effectiveness of different treatments for asthenozoospermia remains uncertain. Hence, by using bioinformatics techniques, the present study aimed to determine the underlying genetic markers and pathogenetic mechanisms associated with asthenozoospermia due to abnormal spermatogenesis and inflammation of the reproductive tract. GSE160749 dataset was downloaded from the Gene Expression Omnibus database, and the data were filtered to obtain 1336 differentially expressed genes (DEGs) associated with asthenozoospermia. These DEGs were intersected with the epithelial mesenchymal transition datasets to yield 61 candidate DEGs. Gene Ontology and Kyoto Encyclopedia of Genes and Genomes pathway enrichment analyses were performed, and the results revealed that these candidate DEGs were significantly enriched in the enzyme-linked receptor pathway and the thyroid hormone pathway. A protein-protein interaction network was constructed to identify the key genes of asthenozoospermia. A total of five key genes were identified, among which *SOX9* was significantly upregulated, while *HSPA4*, *SMAD2*, *HIF1A* and *GSK3B* were significantly downregulated. These findings were validated by conducting reverse transcription-quantitative PCR for clinical semen samples. To determine the underlying molecular mechanisms, a regulatory network of transcription factors and miRNA-mRNA interactions was predicted. The expression levels of *HSPA4*, *SMAD2* and *GSK3B* were positively associated with several related etiological genes of asthenozoospermia. In total, five key genes were closely associated with the level and type of immune cells; higher levels of activated B cells and CD8 T cells were observed in asthenozoospermia. Thus, the findings of the present study may provide clues to determine the underlying novel diagnostic genetic markers and treatment strategies for asthenozoospermia.

Introduction

Male infertility is a complex reproductive disorder caused by hereditary, physiological, pathological and environmental factors. According to a 2018 estimate, male infertility affects 8-12% of couples globally, with the male factor dominating in ~50% of the cases (1). Semen analysis is the key method to diagnose male infertility. The 6th edition of the World Health Organization (WHO) laboratory manual for examining and processing human semen has recently updated the sperm vitality criterion during semen analysis. Sperm vitality is estimated by assessing the membrane integrity of the cells, and it should be tested examined sperm motility is <40%. The reasons for decreased sperm vitality include structural defects in the sperm flagellum, epididymal defects and immunological reactions due to infection (2).

Asthenozoospermia is one of the most common types of male infertility (1), and it is characterized by low sperm motility. A retrospective study conducted in 2018 on 117,979 male semen samples collected from 1989 to 1993 revealed that the incidence of male infertility was 45%, which included asthenozoospermia (11%), oligozoospermia (22%) and azoospermia (12%) as the main causes (3). Asthenozoospermia can also coexist with oligozoospermia and teratozoospermia. In a multicenter study in 2001 (4), the incidence of asthenozoospermia, oligozoospermia or asthenoteratozoospermia, and oligoasthenoteratozoospermia was 2- to 3-fold, 5- to 7-fold, and 16-fold higher, respectively, in the infertile group compared with the normal group.

Several pathogenic factors can influence the development of asthenozoospermia, such as increased scrotal temperature due to varicocele and renal and adrenal metabolite reflux, which can effectively induce apoptosis of genital cells through enhanced oxidative stress. An imbalance in the levels of reactive oxygen species (ROS) and antioxidants can induce anomalous changes in sperm morphology and vitality through fatty acid oxidation of the sperm cell membrane (5). The presence of cysts in the reproductive tract (for example, in the ejaculatory duct and seminal vesicles) can lead to low

Correspondence to: Professor Hongli Yan, Reproductive Medicine Center, The First Affiliated Hospital of Naval Medical University, 168 Changhai Road, Shanghai 200433, P.R. China
E-mail: hongliyan@smmu.edu.cn

Key words: asthenozoospermia, bioinformatics techniques, genetic markers, spermatogenesis, reproductive organ inflammation, immune cells

semen volume and asthenozoospermia due to compression or blockage of the ejaculatory duct (6).

Numerous factors, including immunological, genetic, microbial, physiological and environmental factors, affect sperm health. An imbalance or damage to the immune system in humans can cause sperm antigens to stimulate the production of anti-sperm antibodies, resulting in sperm agglutination and asthenozoospermia (7). Genetic mutations can cause structural and functional changes in microtubules of the sperm flagella, resulting in multiple morphological abnormalities of the sperm flagella and cilia and leading to primary ciliary dyskinesia (8). *Escherichia coli*, *Chlamydia trachomatis* and *Ureaplasma urealyticum* can infect the reproductive system, particularly the accessory gonads, causing inflammation and leukocytosis in the reproductive system. Furthermore, the abundant content of peroxidase in the cytoplasm of leukocytes accelerates ROS production and enhances oxidative stress reactions. These microbial and biochemical effects can damage sperm quality, sperm integrity, and the secretory function of accessory gonadal structures, resulting in a decline in sperm viability (9). The decline in semen volume, sperm concentration and viability, and normal sperm rate is also associated with long-term exposure to polluted air (10). Environmental exposure to heavy metals (such as Pb and Cd) and plasticizers (such as phthalate) can induce DNA damage. Moreover, excessive use of synthetic rubber or polyester can cause a high environmental concentration of bisphenol A, which damages the integrity of sperm DNA. Tobacco metabolites (including nicotine, Cd and benzopyrene) can damage sperm DNA, while alcohol can accelerate the apoptosis of sperm cells (11-13).

Although the effects of physiological and pathological changes, environmental conditions, lifestyle and other exposure factors on male fertility have been progressively confirmed by numerous studies, asthenozoospermia remains a poorly understood disorder because of its complex pathogenetic mechanism and ambiguous treatment effects. Hence, the investigation of sperm quality is critical to improve male fertility. Bioinformatics combines molecular biology techniques and information technology to study the molecular mechanisms of diseases. In the present study, bioinformatics techniques were utilized to elucidate the underlying genetic markers and pathogenetic mechanisms associated with asthenozoospermia. Differentially expressed genes (DEGs) were obtained using the GSE160749 dataset, a newly updated sperm transcriptome profile of infertile men, from the Gene Expression Omnibus (GEO) database (last updated: November 05, 2021). Furthermore, epithelial-mesenchymal transition (EMT) is known to influence embryo and organ development, inflammatory injury and organ repair. Therefore, the obtained DEGs were intersected with EMT datasets to filter candidate DEGs of asthenozoospermia. Subsequently, bioinformatics techniques were used to analyze the key genes, pathways, transcription regulation, immune regulation and other factors involved in asthenozoospermia. These results could enable providing novel clues to treat asthenozoospermia.

Materials and methods

Dataset selection and analysis of DEGs. The GSE160749 dataset (GPL17692, [HuGene-2_1-st] Affymetrix Human Gene 2.1 ST Array [transcript (gene) version]) was downloaded from the GEO database. A total of six fertile control sample files and five asthenozoospermia sample files were selected from this dataset (https://www.ncbi.nlm.nih.gov/geo/query/acc.cgi?acc=GSE160749). The EMT datasets (1184 EMT-related genes) were downloaded from the dbEMT2 database (http://www.dbemt.bioinfo-minzhao.org/dbemt2.txt). DEGs from the GSE160749 dataset were filtered using the limma package (v3.42.2) (14) in R software (v3.6; https://cran.r-project.org/bin/windows/base/old/3.6.0/) based on the following preset thresholds: |log Fold Change| >1.0 and P<0.05. Venn analysis was used to filter the candidate DEGs that intersected with the EMT datasets. The study design and data processing are demonstrated in Fig. 1.

Functional enrichment analyses of the candidate DEGs. To investigate the biological functions and pathways of the candidate DEGs, Gene Ontology (GO) and Kyoto Encyclopedia of Genes and Genomes (KEGG) pathway enrichment analyses were performed using the clusterProfiler package (v4.1.4) in R software (15) (P<0.05). The Metascape database (www.metascape.org) was also used to analyze the candidate DEGs. The preset thresholds of functional enrichment were min overlap ≥3 and P≤0.01.

Construction of the protein-protein interaction (PPI) network. A PPI network was constructed by using the STRING database (https://www.string-db.org/) to determine the correlations among the candidate DEGs. To identify the key genes in asthenozoospermia, the candidate DEGs were filtered based on the constructed PPI network by using the Mcode function of Cytoscape software (v3.7; https://cytoscape.org/). The confidence level was set at 0.5.

Key gene pathway enrichment analysis. By using predefined gene sets, gene set enrichment analysis (GSEA) ranks genes according to their expression patterns in two groups and then checks whether the predefined gene set is overrepresented at the top or bottom of the gene rankings. In the present study, the GSEA database (https://www.gsea-msigdb.org/) was used to find the enriched key gene pathways in asthenozoospermia, and the molecular mechanisms of the key genes were determined. To compare the variations in the enriched KEGG pathways between the control and asthenozoospermia groups, the number of permutations was preset to 1,000, and type was the inputted phenotype.

Transcription factor motif enrichment based on key genes. RcisTarget package (v1.6.0) in R software was utilized (16), to analyze transcription factors (TFs). DNA motifs with significant over-representation in the transcription start site of the genes in the gene set were selected using a database containing genome-wide cross-species rankings for each motif. The selected motifs were then annotated to TFs, and those with a high normalized enrichment score (NES) were retained. Briefly, the area under the curve (AUC) of the motif-motif set pair was computed to estimate the overexpression of each motif in the gene set. This was calculated from the recovery curves of the gene sets used for the ordering of motifs. The NES for each motif was estimated from the AUC

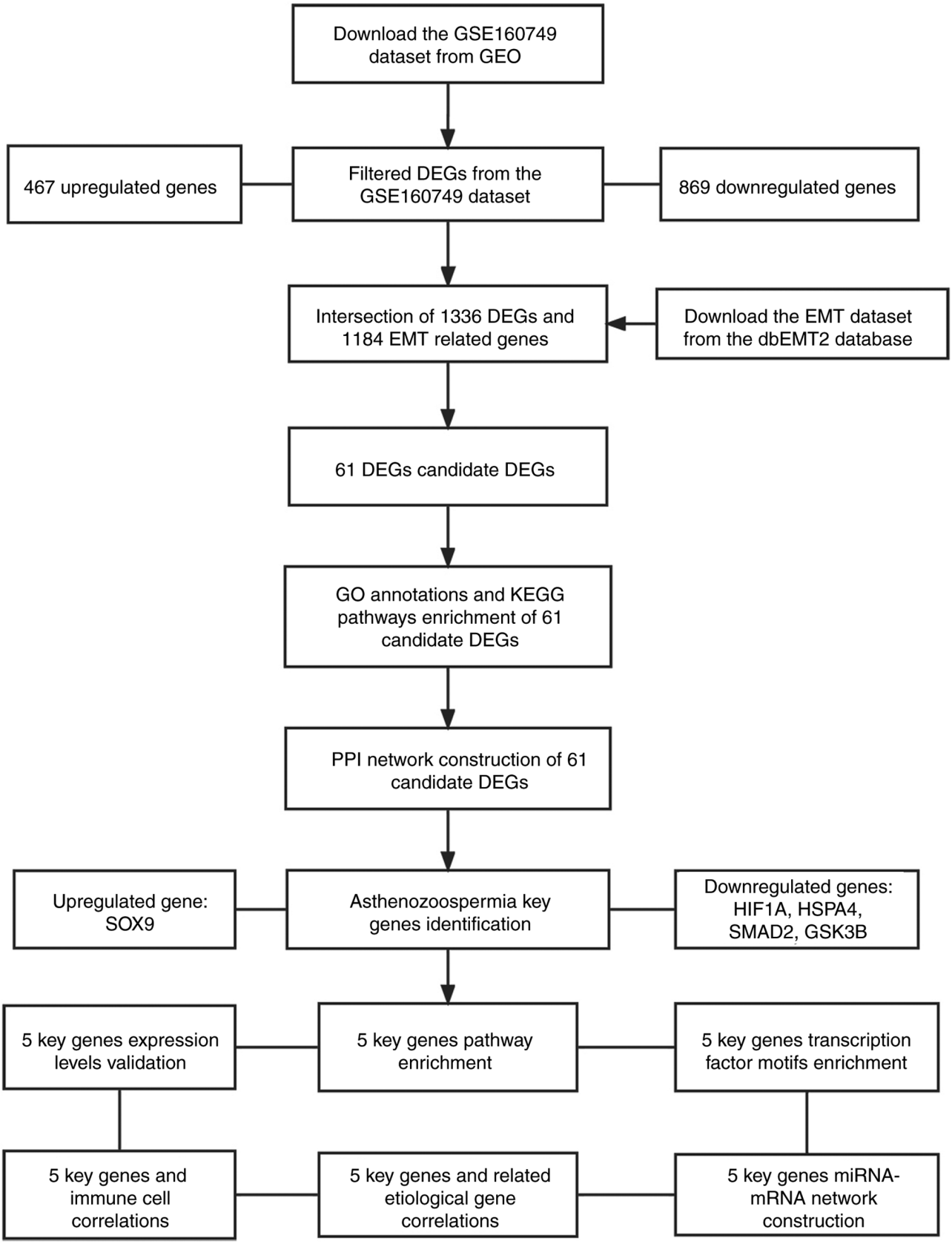

Figure 1. Flowchart of study design and data processing. GEO, Gene Expression Omnibus; DEGs, differentially expressed genes; EMT, epithelial-mesenchymal transition; GO, Gene Ontology; KEGG, Kyoto Encyclopedia of Genes and Genomes; PPI, protein-protein interaction; miRNA, microRNA.

distribution of all motifs in the gene set. In the present study, the 4.6-kb motif (rcistarget.hg19.motifdb.cisbpont.500bp) was used, which is applied to human TFs in the gene-motif ranking database.

miRNA-mRNA network construction based on key genes. To analyze the asthenozoospermia regulatory mechanisms, the miRWalk database (http://129.206.7.150/) was advised to extract miRNA-mRNA pairs. The obtained results were then entered in the TargetScan (https://www.targetscan.org/) or miRDB database (http://www.mirdb.org/). The miRNA-mRNA network was constructed using Cytoscape software (v3.7).

Correlations between key genes and related etiological genes. Related etiological genes (relevance score: top 20) of asthenozoospermia were obtained from the GeneCards database (https://www.genecards.org/). Pearson's correlation analysis was performed to determine the correlations between the key genes and the related etiological genes.

Correlations between key genes and immune cells. The ssGSEA package in R software was used to analyze the proportion and type of immune cells in the semen based on six fertile control sample files and five asthenozoospermia sample files in the GSE160749 dataset. Pearson's correlation analysis was used to analyze the correlations among the key genes and multiple immune cells.

Clinical semen sample collection and validation by reverse-transcription quantitative PCR (RT-qPCR). The present study was approved (approval no. chrec-2018-6) by the Ethics Committee of the Chinese Naval Medical University (Shanghai, China) and was performed in accordance with the principles of the Declaration of Helsinki as revised in 2013. Informed consent was obtained from all participants before sample collection. All patients were Han Chinese with no genetic association. Patients without diseases of the reproductive system (e.g., tumor, inflammation, and varicocele) were included in the healthy control group. Semen samples were collected from 8 healthy individuals and 8 asthenozoospermia patients diagnosed in The First Affiliated Hospital of Naval Medical University (Shanghai, China) in April 2023. Clinicopathological parameters including age distribution are presented in Table II. The samples were obtained through masturbation after 2 to 7 days of abstinence. The samples were processed according to the guidelines of the WHO Laboratory Manual on Human Semen Examination and Processing (6th Edition 2021), and the 5th percentile of the semen parameter values was chosen as the lower reference limit (2). The following parameters were considered for asthenozoospermia semen samples: Samples collected at ≥2 different time points and sperm progressive motility (PR) <30%. The following parameters were considered for normal semen samples: Semen volume ≥1.4 ml, sperm concentration ≥16x10^6/ml, pH≥7.2, PR≥0%, and PR + non-progressive motility (NP) ≥42%.

In the validation test, by using phosphate buffered saline and somatic cell lysis buffer successively, seminal plasma was removed and somatic cells from the semen and extracted pure sperm cells from the samples (17). Subsequently, TRIzol® reagent (Invitrogen; Thermo Fisher Scientific, Inc.) was selected to extract RNA from sperm cells. A commercial kit (cat. no. AG11706; Hunan Accurate Bio-Medical Co., Ltd.) was used for the reverse transcription of RNA into cDNA according to the manufacturer's instructions. The SYBR qPCR mix kit (cat. no. AG11702; Hunan Accurate Bio-Medical Co., Ltd.) was used for RT-qPCR with glyceraldehyde-3-phosphate dehydrogenase (*GAPDH*) as a reference gene. The primers (Sangon Biotech Co., Ltd.) for five target genes are listed in Table I. A total of 20 μl reaction mixture volume was used for RT-qPCR performed with the ABI PRISM 7500 Real-Time PCR System (Applied Biosystems; Thermo Fisher Scientific, Inc.). The qPCR conditions were as follows: Stage 1, initial denaturation at 95˚C for 2 min; Stage 2, 40 cycles of denaturation at 95˚C for 30 sec, annealing at 60˚C for 30 sec, and elongation at 72˚C for 30 sec. All samples were normalized according to *GAPDH* expression, and the relative expression of these genes was quantified using the $2^{-\Delta\Delta Cq}$ method (18).

Table I. Primers used in reverse transcription-quantitative PCR.

No.	Gene name	Primer sequence (5'→3')
1	SOX9	F: AAGCTCTGGAGACTTCTGAACG
		R: CTGCCCGTTCTTCACCGACT
2	HSPA4	F: GTGGACCTGCCAATCGAGAA
		R: CCTCCACTGCGTTCTTAGCA
3	SMAD2	F: TGGGGACTGAGTACACCAAA
		R: GGGATACCTGGAGACGACCA
4	HIF1A	F: TTTGGCAGCAACGACACAGA
		R: TTTCAGCGGTGGGTAATGGA
5	GSK3B	F: TGTGTGTTGGCTGAGCTGTT
		R: TCCCTTGTTGGAGTTCCCAG

F, forward; R, reverse.

Statistical analysis. All the experimental data were recorded in Excel 2007 (Microsoft Corp.). SPSS version 28.0 (IBM Corp.) was used to compare the data between the semen parameters of the normal and asthenozoospermia groups. All measurement data are presented as the mean ± standard deviation which represent the average level and dispersion tendency. The unpaired t-test was performed for comparison between measurement data from clinical semen sample parameter detection and RT-qPCR validation in the normal and asthenozoospermia groups. The DEGs were determined using the Benjamini-Hochberg method. The Pearson's method was performed to analyze the correlation between the expression levels of five key genes and the top 20 related etiological genes in asthenozoospermia. The Wilcoxon rank-sum test and Pearson's method were used to analyze the differential expression levels and correlations of immune cells in six fertile control sample files and five asthenozoospermia sample files from the GSE160749 dataset. For all results, P<0.05 was considered to indicate a statistically significant difference.

Results

Filtered DEGs. A total of 1,336 DEGs were successfully filtered from the GSE160749 dataset (Fig. 2A and B); these DEGs comprised 467 upregulated genes (Table SI) and 869 downregulated genes (Table SII). In total, 61 candidate DEGs

Table II. Age and semen parameters in normal and asthenozoospermia groups.

No.	Parameters	Normal (n=8)	Asthenozoospermia (n=8)	P-value
1	Age	31.75±3.45	33.88±3.83	0.390
2	Semen volume (ml)	4.39±1.52	3.31±1.68	0.220
3	pH	7.20	7.20	NA
4	Sperm concentration (x10^6/ml)	78.24±35.42	19.32±16.12	0.005
5	Progressive motility (%)	70.38±5.93	4.75±4.56	<0.001
6	Motility (%)	75.88±4.52	11.00±9.35	<0.001

The unpaired t-test was used to compare the parameters between the normal and asthenozoospermia groups.

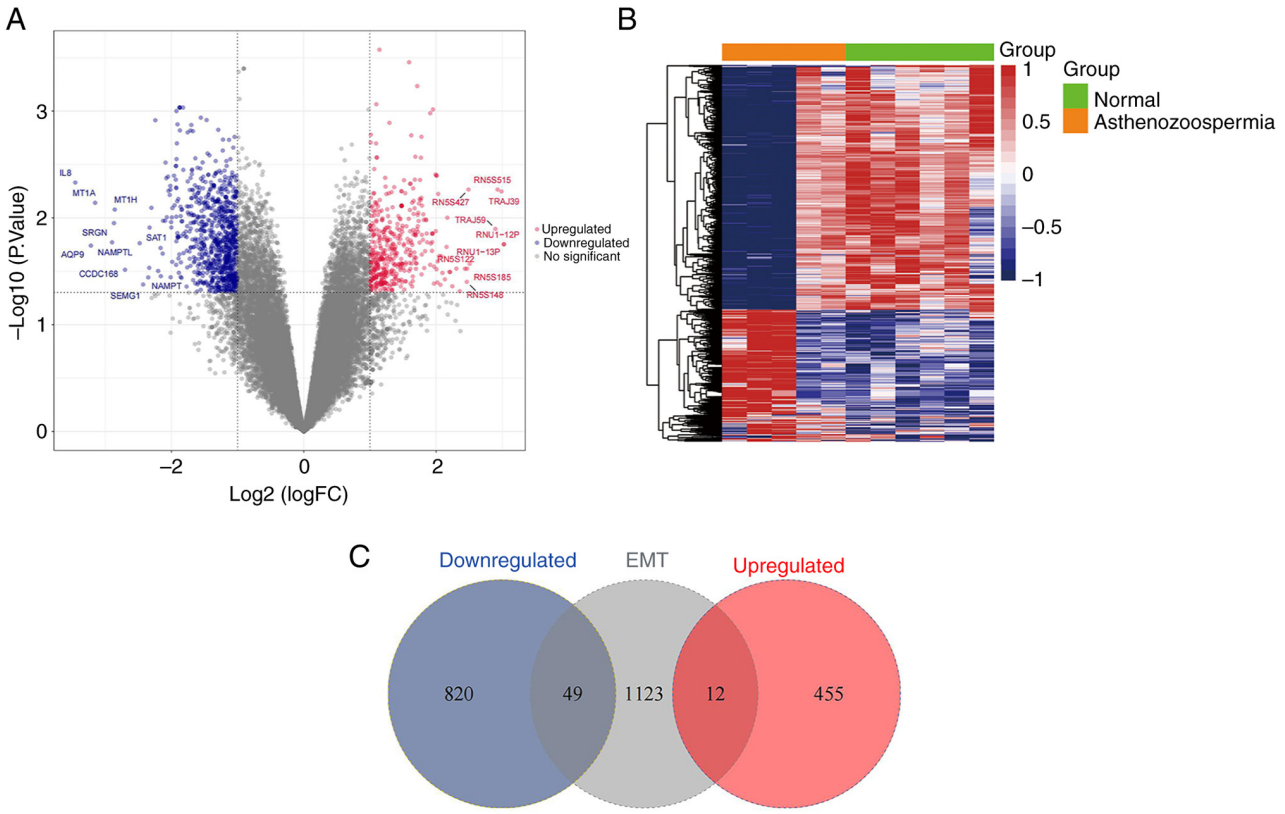

Figure 2. Filtered DEGs from the GSE160749 and EMT datasets. (A) Volcano plot of 1,336 DEGs in six fertile control samples and five asthenozoospermia samples of the GSE160749 dataset. The red points represent upregulated DEGs, the blue points represent downregulated DEGs, and the gray points represent no significant DEGs. X-axis represents fold change, and the farther point from the center with the greater significant difference; Y-axis represents -log10 (P-value) results, and the closer point to the top with the greater significant difference. (B) Heatmap of 1,336 DEGs in six fertile control samples and five asthenozoospermia samples of the GSE160749 dataset. The X-axis represents the samples and the Y-axis represents the genes. The red and blue rectangles respectively represent upregulated and downregulated genes. The deeper red colors indicate the higher expression of genes, the deeper blue colors indicate the lower expression of genes. The black connecting lines indicate the clustering relation among the genes. (C) Venn analysis of the upregulated (red) and downregulated (blue) DEGs intersected with the EMT datasets (gray). DEGs, differentially expressed genes; EMT, epithelial-mesenchymal transition.

that intersected with the EMT datasets were filtered for analysis, which included 12 upregulated genes and 49 downregulated genes (Fig. 2C).

Functional enrichment of the candidate DEGs. GO and KEGG pathway enrichment analyses were conducted to determine functional enrichment of the 61 candidate DEGs (Fig. 3A and B). In the biological processes' category, the 61 DEGs were significantly enriched in the regulation of binding. In the cellular components' category, the DEGs were significantly enriched in the TF complex. In the molecular functions' category, the DEGs were significantly enriched in SMAD binding and hormone receptor binding. Additionally, the pathways that were significantly enriched in the 61 DEGs were the thyroid hormone signaling pathway, TGF-β signaling pathway and Th17 cell differentiation pathway. The Metascape database was also used to determine pathway enrichment of the 61 DEGs. The results demonstrated that the pathways were mainly enriched in the enzyme-linked receptor protein signaling pathway and RNA polymerase II-specific DNA binding TF binding (Fig. 3C).

Figure 3. Enrichment analysis of the 61 candidates DEGs. (A) GO annotations of the 61 candidate DEGs. The X-axis represents the count of enrichment genes. (B) KEGG pathway enrichment analysis of the 61 candidate DEGs. The X-axis represents the count of enrichment genes. (C) Metascape database pathway enrichment analysis of the 61 candidate DEGs. The X-axis represents -log10 (P-value) results; the greater result indicates that the pathway is more significant. DEGs, differentially expressed genes; GO, Gene Ontology; KEGG, Kyoto Encyclopedia of Genes and Genomes; BP, biological process; CC, cellular component; MF, molecular function.

Construction of the PPI network. To conduct in-depth analysis of the relationship among the 61 candidate DEGs, a PPI network was constructed that included 40 nodes and 80 edges (Fig. 4). It is necessary to explain that each node represents a protein and each edge represents a link with two proteins, indicating functional association between proteins. The gene cluster with the highest score was identified from the PPI network by using the MCODE function. The gene cluster included *HSPA4*, *SOX9*, *SMAD2*, *HIF1A* and *GSK3B* (score=5.00), there was five nodes and 10 edges. *SOX9* was upregulated, while *HSPA4*, *SMAD2*, *HIF1A* and *GSK3B* were downregulated in asthenozoospermia.

Validation of clinical semen samples by RT-qPCR. The age and semen parameters in the normal and asthenozoospermia groups are listed in Table II. The RT-qPCR results revealed that

Table III. Normalized enrichment score of the top 3 motifs enrichment.

No.	Motif	NES score	Area under the curve	TF_highconf	Annotation information	Enriched genes
1	cisbp_M6373	6.92	0.648	NFYC (direct Annotation)	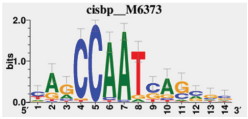	GSK3B, HIF1A, SMAD2, SOX9
2	cisbp_M6537	6.91	0.647	YBX1 (direct Annotation)	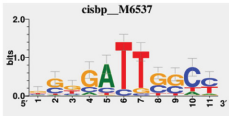	GSK3B, HIF1A, SMAD2, SOX9
3	cisbp_M2301	6.78	0.636	NFYB (direct Annotation)	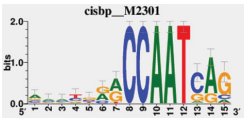	GSK3B, HIF1A, SMAD2, SOX9

Table IV. Co-regulators of the five key genes in the miRNA-mRNA network.

No.	Genes	miRNAs
1	HSPA4, SMAD2 and GSK3B	hsa-miR-8085, hsa-miR-6788-5p
2	SOX9, GSK3B	hsa-miR-4306
3	SOX9, SMAD2	hsa-miR-8485, hsa-miR-5195-3p
4	HSPA4, SMAD2	hsa-miR-30c-2-3p
5	HIF1A, SMAD2	hsa-miR-3121-3p, hsa-miR-6807-5p
6	GSK3B, SMAD2	hsa-miR-3190-3p, hsa-miR-4728-5p, hsa-miR-30c-1-3p, hsa-miR-6881-3p, hsa-miR-5002-5p, hsa-miR-4768-5p, hsa-miR-6731-5p, hsa-miR-6733-5p, hsa-miR-6833-3p, hsa-miR-641, hsa-miR-5584-5p, hsa-miR-6513-3p, hsa-miR-6766-3p

miRNA, microRNA; hsa, *Homo sapiens*.

the expression levels of *HIF1A*, *HSPA4*, *SMAD2* and *GSK3B* (Fig. 5A-D, respectively) were lower in the asthenozoospermia group than in the normal group; however, *SOX9* (Fig. 5E) expression was significantly higher in the asthenozoospermia group. The validation results of the 16 clinical semen samples were consistent with those of the bioinformatics analysis for downregulated and upregulated genes. The Cq values for RT-qPCR validation for clinical semen samples are included in Table SIII.

Key gene pathway enrichment. Pathway enrichment analysis was performed using GSEA on five key genes of asthenozoospermia. *HIF1A* was enriched mainly in the adipocytokine cytokine signaling pathway, JAK-STAT signaling pathway and retinol metabolism (Fig. 6A). *HSPA4* was enriched mainly in aminoacyl tRNA biosynthesis and the tricarboxylic acid (TCA) cycle (Fig. 6B). *SMAD2* was enriched mainly in α-linolenic acid metabolism, glycosylphosphatidylinositol GPI anchor biosynthesis and the renin-angiotensin system (Fig. 6C). *GSK3B* was enriched mainly in α-linolenic acid metabolism, the cell cycle and the renin-angiotensin system (Fig. 6D). *SOX9* was enriched mainly in ABC transporters, α-linolenic acid metabolism, and glycine serine and threonine metabolism (Fig. 6E).

TF motif enrichment for key genes. A total of five key genes were selected from the gene set to analyze their regulation mechanisms. These genes were regulated by multiple TFs. Therefore, cumulative recovery curves were used to enrich these TFs (Fig. 7). The analysis demonstrated that the motif with the highest NES value (6.92) was cisbp_M6373. In total, four genes, namely *GSK3B*, *HIF1A*, *SMAD2* and *SOX9*, were enriched in this motif. TFs of the key genes were identified in all enriched motifs (Tables III and SIV).

miRNA-mRNA network construction for key genes. Several miRNA-mRNA pairs were associated with the mRNAs of the five key genes. A total of 384 miRNA-mRNA pairs (Table SV) were retained from the TargetScan and miRDB databases, including five mRNAs and 361 miRNAs. In this network, 21 miRNAs acted as coregulators among the five key genes (Table IV).

Correlations between key genes and related etiological genes. A correlation analysis was performed between the expression levels of five key genes and the top 20 related etiological genes in asthenozoospermia. *HSPA4*, *SMAD2* and *GSK3B* revealed

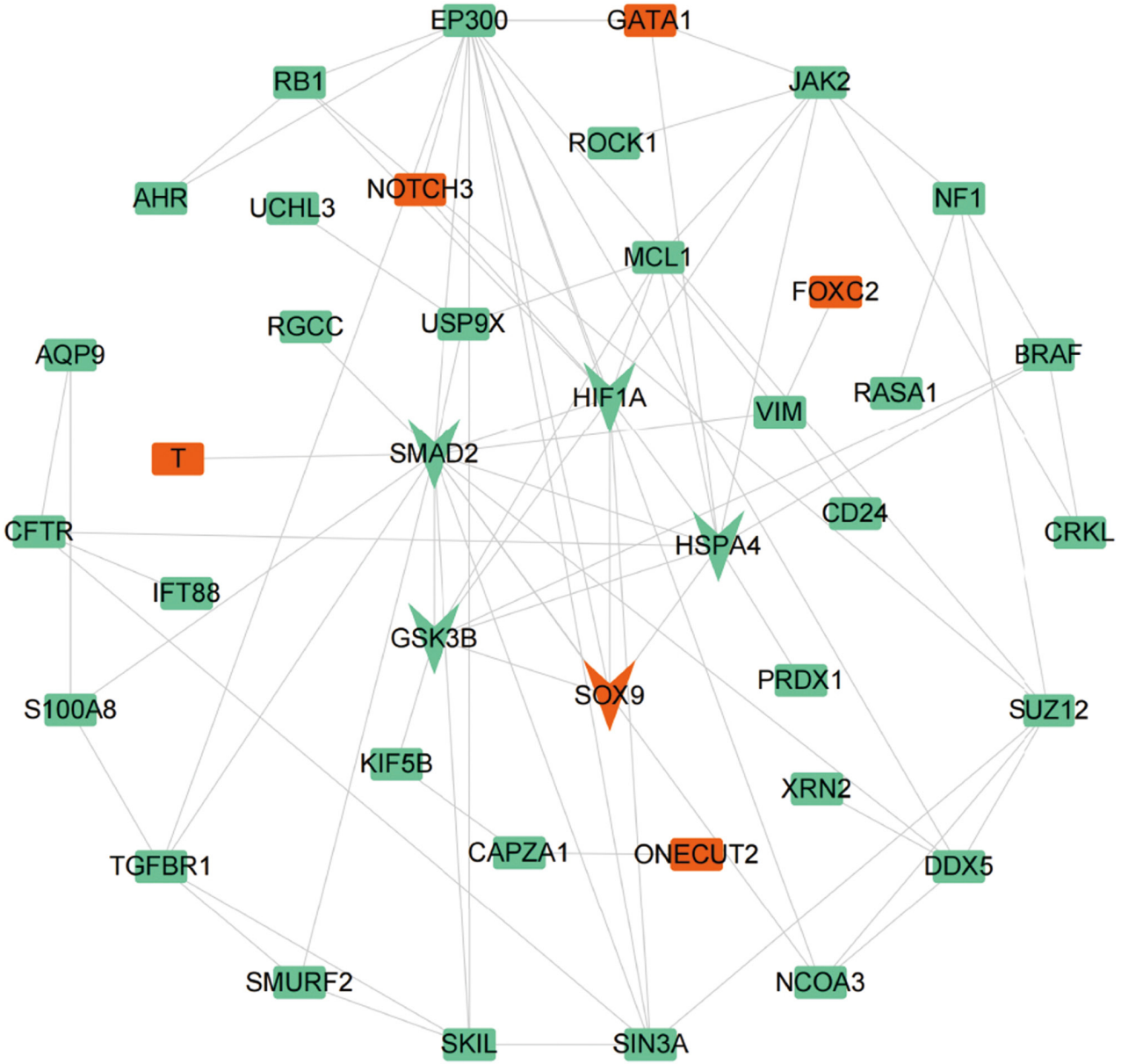

Figure 4. Construction of a PPI network for the differentially expressed genes of 61 candidates. There are 40 nodes and 80 edges in the PPI network. Each node represents a protein, the orange and green colors respectively indicate upregulated and downregulated genes. Each edge represents a link with two proteins, indicating the functional association between proteins. *HIF1A, HSPA4, SOX9, GSK3B*, and *SMAD2* is the highest score cluster (score=5.00) which include five nodes and 10 edges. PPI, protein-protein interaction.

a positive correlation with multiple related etiological genes, including *SMAD2* and *GALNTL5* (r=0.937, P<0.001) and *GSK3B* and *ARMC2* (r=0.928, P<0.001) (Fig. 8 and Table SVI).

Correlations between key genes and immune cells. The correlations of immune cells in six fertile control sample files and five asthenozoospermia sample files from the GSE160749 dataset were analyzed (Fig. 9A). Higher levels of activated B cells and activated CD8 T cells were observed in the five asthenozoospermia samples than in the six control samples (Fig. 9B). Correlations among the expression levels of the five key genes and multiple immune cells were also analyzed in 11 semen samples from the GSE160749 dataset. The expression levels of *HSPA4*, *SMAD2* and *GSK3B* were positively correlated with activated CD4 T cells and effector memory CD4 T cells but negatively correlated with activated B cells and type 17 T helper cells. The *HIF1A* expression level was positively correlated with numerous immune cells, such as activated CD4 T cells, central memory CD4 T cells, central memory CD8 T cells and natural killer (NK) cells. The expression level of *SOX9* was positively correlated with CD56 (bright or dim) NK cells (Fig. 9C).

Discussion

Asthenozoospermia is mainly characterized by poor sperm motility in clinical examination, and it is generally caused by defects in the function or structure of sperms and abnormal spermatoplasm (19). Studies investigating the molecular mechanisms of asthenozoospermia may help discover more

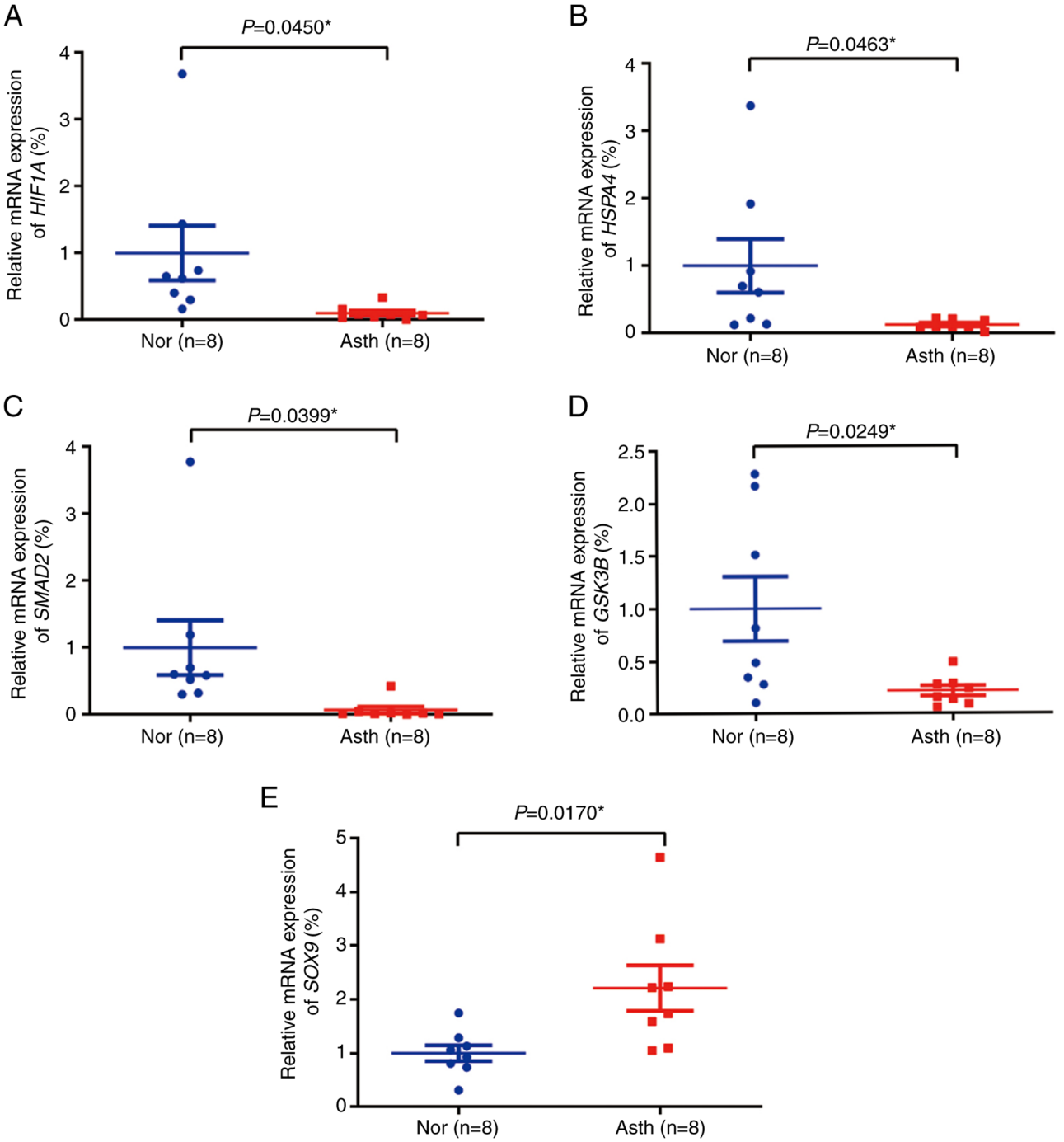

Figure 5. Reverse transcription-quantitative PCR validation of the expression of the five key genes in the clinical semen samples. The unpaired t-test was used to compare the expression of the five key genes between Nor and Asth. (A) *HIF1A*. (B) *HSPA4*. (C) *SMAD2*. (D) *GSK3B*. (E) *SOX9*. Nor, normal group; Asth, asthenozoospermia group.

novel effective treatments for male infertility. Abnormal spermatogenesis and reproductive tract infections are the main causative factors of asthenozoospermia. The critical roles of EMT in embryo and organ development, inflammatory injury, and organ repair have received widespread attention. Cunha *et al* (20) reported the presence of an androgen-receptor (AR)-positive testicular medulla in the developing human testis; this medulla acted as a zone of mesenchymal to epithelial transition and a zone from which AR-positive cells appeared to migrate into the human testicular cortex. The human testicular medulla is a known source of Sertoli cells in seminiferous cords. Klein *et al* (21) noted that dexamethasone therapy improved the outcomes of mice with preclinical uropathogenic E. coli-induced epididymitis and found that EMT was involved in the interstitial fibrosis transformation process of this epididymitis. Therefore, in the present study, the dbEMT2 database was selected to explore the pathogenic genes related to asthenozoospermia. The GSE160749 dataset from the GEO database is a recently updated sperm transcriptome profile of samples from infertile men, and it includes five asthenozoospermia files, seven asthenoteratozoospermia files, six infertile files and six fertile control sample files. A

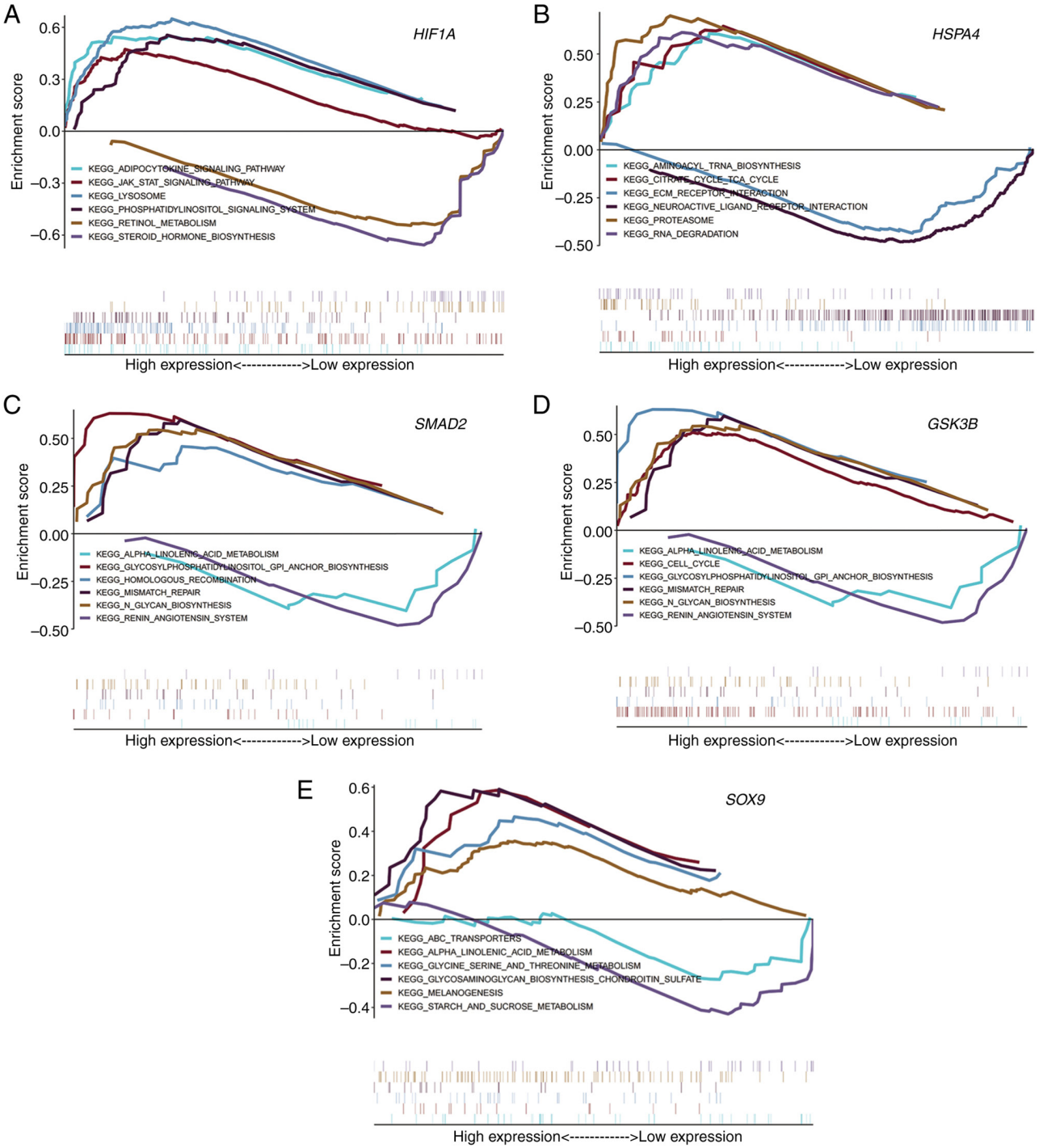

Figure 6. Pathway enrichment analysis of the five key genes. Each key gene display six representative KEGG enrichment pathways. The curve above the X-axis indicates that the gene set of the KEGG pathway, where the key gene is located, is highly expressed in the asthenozoospermia group and vice versa, indicating low expression. (A) *HIF1A*. (B) *HSPA4*. (C) *SMAD2*. (D) *GSK3B*. (E) *SOX9*. KEGG, Kyoto Encyclopedia of Genes and Genomes.

PubMed search revealed that a limited number of relevant studies have contributed to this dataset (22). Therefore, in the present study, five asthenozoospermia files and six fertile control sample files were selected as a dataset to analyze novel key genes in asthenozoospermia. Subsequently, by using bioinformatics techniques, 1,336 DEGs associated with asthenozoospermia were identified, including 467 upregulated genes and 869 downregulated genes. Furthermore, 61 EMT-related genes were identified among these 1,336 DEGs, which included 12 upregulated genes and 49 downregulated genes. The STRING database was utilized to construct a PPI network for the 61 candidate DEGs. Five genes were most closely associated with asthenozoospermia after filtering; this included one upregulated gene (*SOX9*) and four downregulated genes (*HSPA4*, *SMAD2*, *HIF1A* and *GSK3B*). Moreover, the bioinformatics analysis results for these five genes were consistent with the RT-qPCR results for the 16 clinical semen samples used for validation. Therefore, these results may provide novel clues regarding the molecular mechanisms of asthenozoospermia.

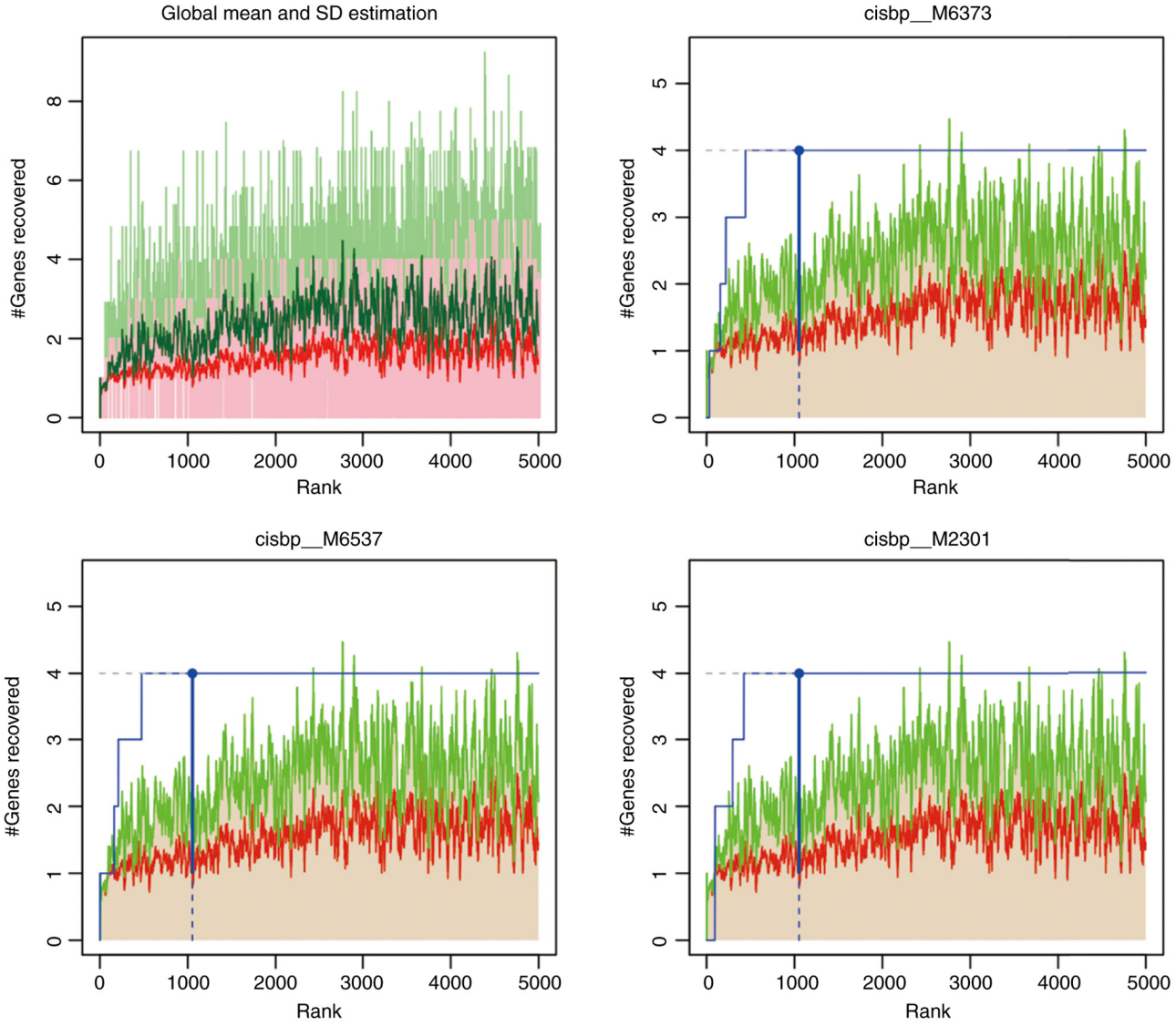

Figure 7. Normalized enrichment score of the top 3 motifs from the cumulative recovery curve. Red line, the global mean of the recovered curve of motif. Green line, mean ± standard deviation. Blue line, the recovered curve of the current motif. Motif is statistically significant when the recovered curve is greater than the mean ± standard deviation.

Among the five key genes, *SOX9*, an autosomal gene and a primary downstream target of SRY, plays a pivotal role in male sexual development. SOX9 is involved in the development or maintenance of Sertoli cells and in gonadal dysgenesis and XY and XX sex reversal (23,24). HSPA4 plays an important role in spermatogenesis and is also involved in the development of oligozoospermia and varicocele (25). Compared with wild-type littermates, Hspa4-deficient mice showed a drastic reduction in the total number of spermatozoa and their motility. The majority of pachytene spermatocytes in juvenile Hspa4$^{(-/-)}$ mice failed to complete the first meiotic prophase and underwent apoptosis (26). SMAD2 is mainly localized in the cytoplasm of meiotic genital, Sertoli and Leydig cells. It plays an important role in testicular development and spermatogenesis (27). HIF1A was robustly expressed in spermatogonial cells of the testis in both juvenile (6 weeks old) and adult (3 months old) male mice (28). Gorga *et al* (29) suggested that HIFs may be involved in regulating the proliferation of Sertoli cells by follicle-stimulating hormone (FSH). However, Ghandehari-Alavijeh *et al* (30) reported a different result for the association of HIF1A expression with asthenozoospermia; these authors found a significant negative correlation between HIF1A expression (r=-0.403, P=0.046) and sperm motility. Therefore, the function of HIF1A in asthenozoospermia will require further investigations. GSK3A and GSK3B are two isomers of GSK3. Both these isomers are related to spermatogenesis and sperm motility, and the effect of GSK3A was found to be more significant than that of GSK3B. Following GSK3A knockout in the testis, testicular weight and sperm counts were normal in GSK3A$^{(-/-)}$ mice; however, the number of infertile male mice increased because of decreased sperm motility. Compared with wild-type mice, GSK3A$^{-/-}$ mice exhibited lower sperm ATP levels and flagellar beat amplitude (31,32). As one of the key downregulated genes in asthenozoospermia, the role of GSK3B in spermatogenesis requires confirmation in future research.

In the present study, several pathways that may provide clues to the molecular mechanisms of asthenozoospermia were

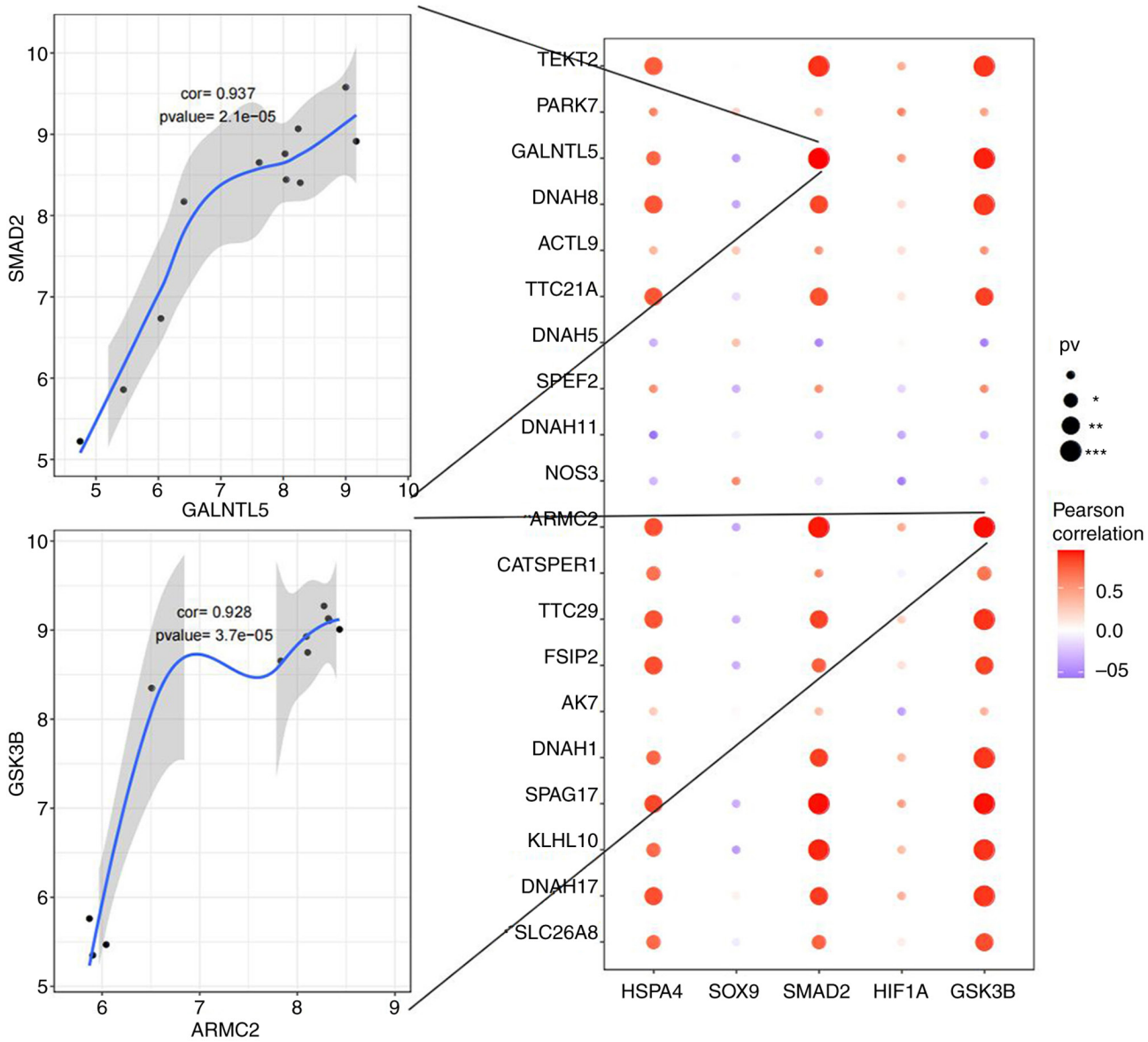

Figure 8. Correlation analysis of the five key genes and the top 20 asthenozoospermia-related etiological genes using Pearson's method. *P<0.05, **P<0.01 and ***P<0.001. Cor, correlation.

identified. The thyroid hormone signaling pathway affects the testis in various ways, including its effects on Leydig cells, Sertoli cells and spermatogenic cells. A surplus or deficiency of thyroid hormone can lead to abnormal testicular function. Hyperthyroidism is associated with decreased semen volume, sperm density, motility and abnormal sperm morphology (33). *In vitro* experiments have revealed that in male patients with idiopathic infertility, 0.9 pmol/l of levothyroxine (LT4) significantly increased the percentage of spermatozoa with high mitochondrial membrane potential and improved sperm motility. LT4 also reduced sperm necrosis and lipid peroxidation, thereby ameliorating chromatin compactness. LT4 exerted these effects at 2.9 pmol/l concentration, which is close to the physiological concentration of free thyroxine (FT4) in the seminal fluid of euthyroid subjects. Thyroid hormones play a beneficial role in sperm mitochondrial function, oxidative stress and DNA integrity (34). In a cross-sectional study of 5401 infertile men, subclinical hypothyroidism was significantly associated with an increased risk of an abnormal DNA fragmentation index (DFI) (35). The enzyme-linked receptor signaling pathway is related to cell reproduction, growth and differentiation processes (36). The enzyme-linked receptor is a transmembrane protein, and the intracellular domain usually exhibits some enzyme activity. Enzyme-linked receptors respond slowly to extracellular signaling (measured in h) and require coordination among numerous intracellular transduction steps. A number of experiments have confirmed that receptor tyrosine kinase (RTK) activity may affect primordial germ cell migration through the RTK-Ras signaling pathway. Mitogen-activated protein kinase (MAPK) can promote genital cell proliferation, meiosis and Sertoli cell proliferation. Differential miRNA expression is associated with the PI3K-AKT and MAPK signaling pathways in asthenozoospermia, and sperm motility is regulated through the concerted efforts of these signaling pathways (37-39). Transforming growth factor-beta (TGF-β)

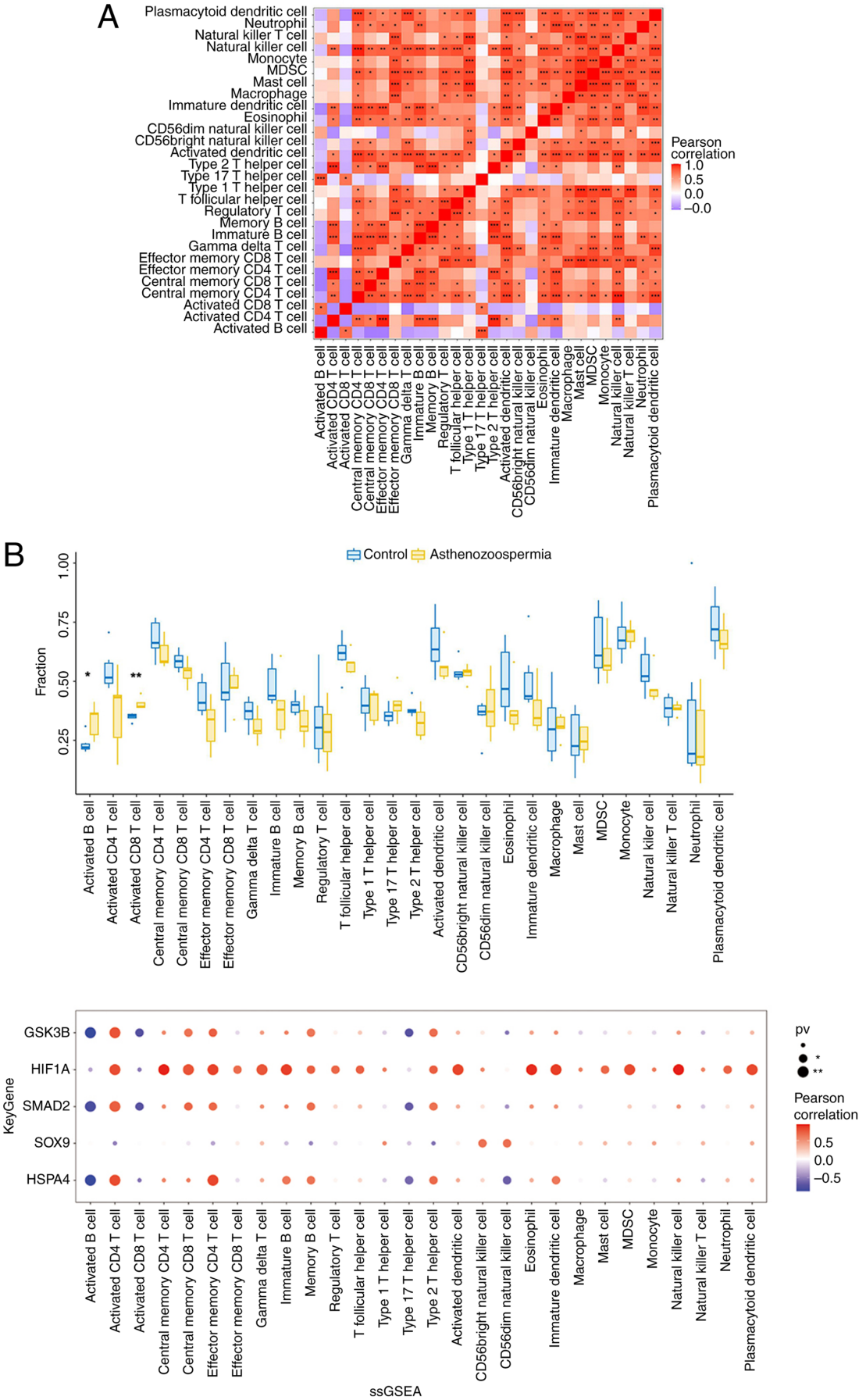

Figure 9. Correlation analysis of the five key genes and immune cells. (A) Correlations of multiple immune cells in the 11 semen samples from the GSE160749 dataset analyzed using Pearson's method. (B) Comparison of the levels of immune cells in the 11 semen samples from the GSE160749 dataset using the Wilcoxon rank-sum test. (C) Correlations of the expression levels of the five key genes and multiple immune cells in the 11 semen samples from the GSE160749 dataset analyzed using Pearson's method. *P<0.05, **P<0.01 and ***P<0.001. ssGSEA, single-sample gene set enrichment analysis.

family members and their receptors are expressed in the testis and play important paracrine and autocrine roles in testicular development and spermatogenesis. SMAD is a downstream protein of the TGF-β family, and the TGF-β-SMAD pathway plays an important role in testicular development and spermatogenesis (27). Inhibin B, a member of the TGF-β family, is involved in the regulation of spermatogenesis. A previous study revealed a high expression of inhibin B in Sertoli cells, Leydig cells, and the cytoplasm of spermatogonia in patients with focal spermatogenesis disorders (40). The JAK-STAT signaling pathway is stimulated by cytokines and plays a role in cell proliferation, differentiation, apoptosis and immune regulation. The JAK-STAT pathway may also be involved in the pathogenic mechanism of asthenozoospermia. The protein and mRNA levels of both Janus kinase (JAK) and signal transducer and activator of transcription (STAT) were significantly reduced in asthenozoospermia (41).

The five identified key genes were also found to be enriched in several other signaling pathways. *HSPA4* was enriched in the TCA cycle. As the common pathway for the catabolism of sugars, lipids and proteins in humans, the TCA cycle is the main pathway of energy production. Recent studies have demonstrated that this pathway is involved in spermatogenesis in asthenozoospermia patients. The semen of asthenozoospermia patients showed decreased expression of four enzymes (fructokinase, citrate synthase, succinate dehydrogenase and spermine synthase) related to energy metabolism (42). The levels of citrate, malate, succinate and pyruvate were substantially decreased; however, lactate levels were increased. These results suggested that asthenozoospermic patients had reduced energy produced by aerobic metabolism through the TCA cycle, which was compensated by the anaerobic glycolytic pathway, resulting in reduced sperm capacity. Isocitrate dehydrogenase 3 is a key enzyme in the mitochondrial TCA cycle, and its reduced levels can cause sperm energy deficits and disrupt acrosome and flagellogenesis, resulting in spermatogenesis arrest (43). Furthermore, extramitochondrial citrate synthase is abundantly found in the sperm head. A metabolomics analysis of aged sperms revealed that the loss of extramitochondrial citrate synthase enhances the TCA cycle in the mitochondria with age, presumably leading to the depletion of extramitochondrial citrate; this might lead to age-dependent male infertility (44).

SOX9, *SMAD2* and *GSK3B* were enriched in the α-linoleic acid metabolic signaling pathway, which can be regarded as the focus of the molecular mechanism in the pathogenesis of asthenozoospermia. The lipid composition of the sperm membrane significantly affects sperm quality and function. Sperm samples from asthenozoospermic patients revealed a lower level of polyunsaturated fatty acids (such as docosahexaenoic acid) and a higher level of saturated fatty acids (such as palmitic acid) than those from normal individuals (45). A randomized controlled study that evaluated the effect of long-term nut consumption on changes in semen parameters reported that nuts were rich in unsaturated fatty acids such as α-linoleic acid, which increased sperm count, vitality, motility and morphology, and the DFI level of sperm was significantly reduced (46). Similar results were obtained in long-term observations of the effects of animal diets on sperm parameters (47). *SMAD2* and *GSK3B* were simultaneously enriched in the renin-angiotensin system (RAS) signaling pathway in the male reproductive system, which regulates male fertility through paracrine and autocrine mechanisms. RAS is present in Leydig, Sertoli and spermatogenic cells in the testis and regulates testosterone and spermatogenesis. Angiotensin-converting enzyme, angiotensin II type 2 receptor and aminopeptidase N in the testicular RAS can be used as potential biological markers of high-quality embryos to assess and diagnose male fertility (48). *SOX9* was enriched in the glycine-serine-threonine metabolism signaling pathway (49). This pathway is activated and affects sperm motility in asthenozoospermia, oligozoospermia, teratozoospermia and azoospermia.

Leptin is a member of the adipocytokine signaling pathway enriched by *HIF1A*. Human and animal studies have identified that leptin correlates with male infertility and obesity. Increased leptin levels are associated with low sperm count, high abnormal sperm count, enhanced sperm oxidative stress effects and obesity (50). Daily intraperitoneal administration of 5-30 mg/kg body weight leptin for 42 days in adult rats decreased the sperm count and increased the fraction of abnormal sperms (51). Obesity-related diseases are associated with dysregulated adipocyte function and microenvironmental inflammatory processes. Dysregulated adipocytokines notably influence the insulin signaling pathway and may induce adverse effects on testicular function (52). Although obesity factors negatively affect sperm quality and function, they can still be transferred as epigenetic factors to the offspring (53). In a previous study, patients with varicocele and leukocytospermia revealed significantly higher seminal plasma leptin levels and sperm apoptosis rates than the control group (54). Seminal plasma leptin levels were significantly associated with the sperm apoptotic rate, and leptin may promote sperm cell apoptosis. It was also discovered that leptin induces sperm cell apoptosis through TNF-α in leukozoospermic patients (54). However, adiponectin and its receptors, expressed in male genital cells, can promote spermatogenesis and maturation (55). Treatment of elderly mice with exogenous adiponectin significantly improved testicular mass, genital cell proliferation, insulin receptor expression, testicular glucose uptake, antioxidant enzyme activity and testosterone synthesis. Thus, adiponectin therapy could serve as an effective therapeutic strategy to improve sperm and testosterone levels in the testis (56). *HIF1A* was also enriched in the retinol signaling pathway. Retinol is also known as vitamin A, and its metabolite retinoic acid (RA) occurs in the seminiferous tubules. RA is stimulated by hormones such as FSH and testosterone and can regulate the processes of proliferation and differentiation of spermatogonia, meiosis, spermiogenesis and sperm release. RA regulates the expression of Stra8, Kit, GDNF and BMP4 to promote or inhibit spermatogenesis through various pathways. RA also inhibits spermatogonial renewal by directly or indirectly inhibiting the expression of DMRT, GDNF and cyclin. RA controls spermatogonial stem cell differentiation through Kit induction and Nanos2 inhibition and regulates spermatogonia meiosis through Stra8 upregulation. At the spermatogenesis stage, RARα binds to RA as a key regulator and upregulates Stra8 to control spermatogenesis. Although RA plays an important role in all stages of spermatogenesis, it has more critical involvement in spermatogonia differentiation

and early meiosis of spermatocytes (57). Although the role of adiponectin and retinol in supporting male reproductive function has been observed in some clinical treatments or in animal studies, the appropriateness of these drugs remains to be validated by more clinical trials and results.

Hernández-Silva *et al* (58) found that human spermatozoa RNA includes both non-coding and protein-coding RNAs that play a potential regulatory function in male fertility. They identified 100 transcripts with consistent differential expression as candidates for the molecular source of asthenozoospermia. As underlying biomarkers, miRNAs may provide evidence of the pathophysiological changes occurring during the spermatogenesis process. Corral-Vazquez *et al* (59) analyzed 48 clinical semen samples to search new molecular biomarkers for diagnosing male infertility, and they finally detected 2 pairs of miRNAs (hsa-miR-942-5p/hsa-miR-1208 and hsa-miR-34b-3p/hsa-miR-93-3p). In the present study, a regulatory network of TFs and miRNAs was analyzed and constructed, and it was proposed that the synergistic effect of these TFs and miRNAs could serve as a novel approach to investigate the underlying mechanisms and molecular targets of asthenozoospermia.

To date, very few studies have investigated the effects of the testis immune microenvironment on asthenozoospermia. As a complete and stable immune microenvironment, the human blood-testis barrier is jointly regulated by humoral and cellular immunity, and immune cells, immunoglobulins and immunoregulatory factors play a coordinated role in maintaining this immune microenvironment. Inflammatory factors and oxidative stress play an etiological role in asthenozoospermia and can stimulate B cell and T cell activation (60-62). This finding is consistent with the results of the present study, where high levels of activated B cells and CD8 T cells were detected in the semen samples of the asthenozoospermia group. Activated B cells can synthesize and secrete immunoglobulins, which are involved in the humoral immune response. As important components in cellular immunity, CD8 T cells mediate cytotoxic effects and play a critical role in infection and inflammation. Based on the GSE160749 dataset, correlations were found among the five identified key genes and different immune cells, thus providing new clues regarding the role of cellular immunity in the mechanism of asthenozoospermia and clinical therapeutic sensitivity. An analysis of seminal leukocyte subsets of 70 sub-fertile men identified that the levels of T (CD3 and CD69), B (CD20 and CD69), NK (CD56) and CD8 T cells were significantly elevated in the oligoasthenospermia group (63). Leukocytospermia may impair sperm function through enhanced helper T-cell regulation. An increase in B cells may induce the secretion of more anti-sperm antibodies, thereby leading to low fertility. NK cells may mediate the entire process of sperm damage. This is consistent with the results obtained for CD4 T, CD8 T and CD56 (bright or dim) NK cells in the present study. These observations suggested that the five identified key genes in asthenozoospermia are strongly associated with the expression of immune cells and play an important regulatory role in the testis immune microenvironment. Furthermore, in the study of the correlations among multiple etiological genes, *HSPA4*, *SMAD2* and *GSK3B* were significantly positively associated with five spermatogenesis-related genes (*SLC26A8*, *GALNTL5*, *ARMC2*, *FSIP2* and *KLHL10*) and eight sperm flagellar function-related genes (*TEKT2*, *DNAH8*, *TTC21A*, *CATSPER1*, *TTC29*, *DNAH1*, *SPAG17* and *DNAH17*). The knowledge of gene interactions in asthenozoospermia is currently limited, and the findings of the present study may provide a new avenue to study the interactions of etiological genes of asthenozoospermia.

Previous studies have suggested that the ordered expression of key genes is crucial during spermatogenesis and that abnormal gene expression may lead to poor sperm quality or functional defects (64-66).

The present study has certain limitations. First, the GSE160749 dataset does not contain abundant sample profiles, which may limit the accuracy of our results to some extent. Second, although bioinformatics evidence suggests that the disturbed expression of the five key genes affects male spermatogenesis and sperm function, additional *in vivo* experiments are required to confirm these results.

In conclusion, in the present study, bioinformatics techniques were used to identify five key genes and signaling pathways. The underlying molecular mechanisms of asthenozoospermia were explored, and correlations were found between the expression of these key genes with multiple related etiological genes and immune cells in patients with asthenozoospermia. These findings could provide clues to identify novel diagnostic genetic biomarkers and treatment strategies for asthenozoospermia.

Acknowledgements

Not applicable.

Funding

The present study was supported (grant. no. 23JSZ03) by the Family Planning Program of Military Medical Innovation Project of Chinese People's Liberation Army.

Availability of data and materials

The data generated in the present study may be found in the Gene Expression Omnibus databased under accession number GSE160749 or at the following URL: https://www.ncbi.nlm.nih.gov/geo/query/acc.cgi?acc=GSE160749 and in the epithelial-mesenchymal transition gene database at the following URL: http://www.dbemt.bioinfo-minzhao.org/dbemt2.txt. The other data generated in the present study may be requested from the corresponding author.

Authors' contributions

YZ and HY designed the present study. JX and YW contributed to the detection of clinical semen sample parameters, the extraction of pure sperm cells and the collection of clinical data. YZ and YP participated in RT-qPCR analysis. YZ, YP, YW and JX drafted the manuscript and prepared figures and tables. YZ, YP, YW, JX and HY revised the paper. YZ and HY confirm the authenticity of all the raw data. All authors have read and approved the final manuscript.

Ethics approval and consent to participate

The present study was approved (approval no. chrec-2018-6) by the Ethics Committee of the Chinese Naval Medical University and was performed in accordance with the principles of the Declaration of Helsinki. Informed consent was obtained from all participants before sample collection.

Patient consent for publication

Not applicable.

Competing interests

The authors declare that they have no competing interests.

References

1. Agarwal A, Baskaran S, Parekh N, Cho CL, Henkel R, Vij S, Arafa M, Panner Selvam MK and Shah R: Male infertility. Lancet 397: 319-333, 2021.
2. WHO-World Health Organization. WHO Laboratory Manual for the Examination and Processing of Human Semen (6th ed). In: Examination and post-examination procedures. WHO. 2021. https://apps.who.int/iris/rest/bitstreams/1358672/retrieve. Accessed 27 Jul, 2021.
3. Mehra BL, Skandhan KP, Prasad BS, Pawankumar G, Singh G and Jaya V: Male infertility rate: A retrospective study. Urologia 85: 22-24, 2018.
4. Guzick DS, Overstreet JW, Factor-Litvak P, Brazil CK, Nakajima ST, Coutifaris C, Carson SA, Cisneros P, Steinkampf MP, Hill JA, *et al*: Sperm morphology, motility, and concentration in fertile and infertile men. N Engl J Med 345: 1388-1393, 2001.
5. Cho CL, Esteves SC and Agarwal A: Novel insights into the pathophysiology of varicocele and its association with reactive oxygen species and sperm DNA fragmentation. Asian J Androl 18: 186-193, 2016.
6. Belet U, Danaci M, Sarikaya S, Odabaş F, Utaş C, Tokgöz B, Sezer T, Turgut T, Erdoğan N and Akpolat T: Prevalence of epididymal, seminal vesicle, prostate, and testicular cysts in autosomal dominant polycystic kidney disease. Urology 60: 138-141, 2002.
7. Li N, Wang T and Han D: Structural, cellular and molecular aspects of immune privilege in the testis. Front Immunol. 3: 152, 2012.
8. Touré A, Martinez G, Kherraf ZE, Cazin C, Beurois J, Arnoult C, Ray PF and Coutton C: The genetic architecture of morphological abnormalities of the sperm tail. Hum Genet 140: 21-42, 2021.
9. Condorelli RA, Russo GI, Calogero AE, Morgia G and La Vignera S: Chronic prostatitis and its detrimental impact on sperm parameters: A systematic review and meta-analysis. J Endocrinol Invest 40: 1209-1218, 2017.
10. Zhang J, Cai Z, Ma C, Xiong J and Li H: Impacts of outdoor air pollution on human semen quality: A meta-analysis and systematic review. Biomed Res Int 2020: 7528901, 2020.
11. Rahman MS, Kwon WS, Lee JS, Yoon SJ, Ryu BY and Pang MG: Bisphenol-A affects male fertility via fertility-related proteins in spermatozoa. Sci Rep 5: 9169, 2015.
12. Pant N, Kumar G, Upadhyay AD, Patel DK, Gupta YK and Chaturvedi PK: Reproductive toxicity of lead, cadmium, and phthalate exposure in men. Environ Sci Pollut Res Int 21: 11066-11074, 2014.
13. Aboulmaouahib S, Madkour A, Kaarouch I, Sefrioui O, Saadani B, Copin H, Benkhalifa M, Louanjli N and Cadi R: Impact of alcohol and cigarette smoking consumption in male fertility potential: Looks at lipid peroxidation, enzymatic antioxidant activities and sperm DNA damage. Andrologia: Nov 21, 2018 (Epub ahead of print).
14. Ritchie ME, Phipson B, Wu D, Hu Y, Law CW, Shi W and Smyth GK: limma powers differential expression analyses for RNA-sequencing and microarray studies. Nucleic Acids Res 43: e47, 2015.
15. Wu T, Hu E, Xu S, Chen M, Guo P, Dai Z, Feng T, Zhou L, Tang W, Zhan L, *et al*: clusterProfiler 4.0: A universal enrichment tool for interpreting omics data. Innovation (Camb) 2: 100141, 2021.
16. Aibar S, Hulselmans G and Aerts S: RcisTarget: Identify transcription factor binding motifs enriched on a gene list. Laboratory of Computational Biology; VIB-KU Leuven Center for Brain & Disease Research. 2016. Available from: https://bioconductor.org/packages/3.12/bioc/html/RcisTarget.html.
17. Goodrich R, Johnson G and Krawetz SA: The preparation of human spermatozoal RNA for clinical analysis. Arch Androl 53: 161-167, 2007.
18. Livak KJ and Schmittgen TD: Analysis of relative gene expression data using real-time quantitative PCR and the 2(-Delta Delta C(T)) Method. Methods 25: 402-408, 2001.
19. Krausz C and Riera-Escamilla A: Genetics of male infertility. Nat Rev Urol 15: 369-384, 2018.
20. Cunha GR, Cao M, Aksel S, Derpinghaus A and Baskin LS: Mouse-human species differences in early testicular development and its implications. Differentiation 129: 79-95, 2023.
21. Klein B, Pant S, Bhushan S, Kautz J, Rudat C, Kispert A, Pilatz A, Wijayarathna R, Middendorff R, Loveland KL, *et al*: Dexamethasone improves therapeutic outcomes in a preclinical bacterial epididymitis mouse model. Hum Reprod 34: 1195-1205, 2019.
22. Chen Y, Sun T, Liu K, Yuan P and Liu C: Exploration of the common genetic landscape of COVID-19 and male infertility. Front Immunol 14: 1123913, 2023.
23. Major AT, Estermann MA and Smith CA: Anatomy, endocrine regulation, and embryonic development of the rete testis. Endocrinology 162: bqab046, 2021.
24. Jedidi I, Ouchari M and Yin Q: Autosomal single-gene disorders involved in human infertility. Saudi J Biol Sci 25: 881-887, 2018.
25. Ferlin A, Speltra E, Patassini C, Pati MA, Garolla A, Caretta N and Foresta C: Heat shock protein and heat shock factor expression in sperm: relation to oligozoospermia and varicocele. J Urol 183: 1248-1252, 2010.
26. Held T, Barakat AZ, Mohamed BA, Paprotta I, Meinhardt A, Engel W and Adham IM: Heat-shock protein HSPA4 is required for progression of spermatogenesis. Reproduction 142: 133-144, 2011.
27. Xu J, Beyer AR, Walker WH and McGee EA: Developmental and stage-specific expression of Smad2 and Smad3 in rat testis. J Androl 24: 192-200, 2003.
28. Takahashi N, Davy PM, Gardner LH, Mathews J, Yamazaki Y and Allsopp RC: Hypoxia inducible factor 1 alpha is expressed in germ cells throughout the murine life cycle. PLoS One 11: e0154309, 2016.
29. Gorga A, Rindone G, Regueira M, Riera MF, Pellizzari EH, Cigorraga SB, Meroni SB and Galardo MN: HIF involvement in the regulation of rat Sertoli cell proliferation by FSH. Biochem Biophys Res Commun 502: 508-514, 2018.
30. Ghandehari-Alavijeh R, Zohrabi D, Tavalaee M and Nasr-Esfahani MH: Association between expression of TNF-α, P53 and HIF1α with asthenozoospermia. Hum Fertil (Camb) 22: 145-151, 2019.
31. Freitas MJ, Silva JV, Brothag C, Regadas-Correia B, Fardilha M and Vijayaraghavan S: Isoform-specific GSK3A activity is negatively correlated with human sperm motility. Mol Hum Reprod 25: 171-183, 2019.
32. Bhattacharjee R, Goswami S, Dudiki T, Popkie AP, Phiel CJ, Kline D and Vijayaraghavan S: Targeted disruption of glycogen synthase kinase 3A (GSK3A) in mice affects sperm motility resulting in male infertility. Biol Reprod 92: 65, 2015.
33. La Vignera S and Vita R: Thyroid dysfunction and semen quality. Int J Immunopathol Pharmacol 32: 2058738418775241, 2018.
34. Condorelli RA, La Vignera S, Mongioì LM, Alamo A, Giacone F, Cannarella R and Calogero AE: Thyroid hormones and spermatozoa: In VitroEffects on Sperm mitochondria, viability and DNA Integrity. J Clin Med 8: 756, 2019.
35. Zhao S, Tang L, Fu J, Yang Z, Su C and Rao M: Subclinical Hypothyroidism and Sperm DNA Fragmentation: A Cross-sectional Study of 5401 men seeking infertility care. J Clin Endocrinol Metab 107: e4027-e4036, 2022.
36. Silver-Morse L and Li WX: The role of receptor tyrosine kinases in primordial germ cell migration. Methods Mol Biol 750: 291-306, 2011.

37. Ni FD, Hao SL and Yang WX: Multiple signaling pathways in Sertoli cells: Recent findings in spermatogenesis. Cell Death Dis 10: 541, 2019.
38. Liang G, Wang Q, Zhang G, Li Z and Wang Q: Differentially expressed miRNAs and potential therapeutic targets for asthenospermia. Andrologia 54: e14265, 2022.
39. Parte PP, Rao P, Redij S, Lobo V, D'Souza SJ, Gajbhiye R and Kulkarni V: Sperm phosphoproteome profiling by ultra performance liquid chromatography followed by data independent analysis (LC-MS(E)) reveals altered proteomic signatures in asthenozoospermia. J Proteomics 75: 5861-5871, 2012.
40. Demyashkin GA: Inhibin B in seminiferous tubules of human testes in normal spermatogenesis and in idiopathic infertility. Syst Biol Reprod Med 65: 20-28, 2019.
41. Li J, Zhang L and Li B: Correlative study on the JAK-STAT/PSMβ3 signal transduction pathway in asthenozoospermia. Exp Ther Med 13: 127-130, 2017.
42. Chen L, Wen CW, Deng MJ, Ping-Li, Zhang ZD, Zhou ZH and Wang X: Metabolic and transcriptional changes in seminal plasma of asthenozoospermia patients. Biomed Chromatogr 34: e4769, 2020.
43. Zhu S, Huang J, Xu R, Wang Y, Wan Y, McNeel R, Parker E, Kolson D, Yam M, Webb B, *et al*: Isocitrate dehydrogenase 3b is required for spermiogenesis but dispensable for retinal viability. J Biol Chem 298: 102387, 2022.
44. Kang W, Harada Y, Yamatoya K, Kawano N, Kanai S, Miyamoto Y, Nakamura A, Miyado M, Hayashi Y, Kuroki Y, *et al*: Extra-mitochondrial citrate synthase initiates calcium oscillation and suppresses age-dependent sperm dysfunction. Lab Invest 100: 583-595, 2020.
45. Eslamian G, Amirjannati N, Rashidkhani B, Sadeghi MR, Baghestani AR and Hekmatdoost A. Dietary fatty acid intakes and asthenozoospermia: A case-control study. Fertil Steril 103: 190-198, 2015.
46. Salas-Huetos A, Moraleda R, Giardina S, Anton E, Blanco J, Salas-Salvadó J and Bulló M: Effect of nut consumption on semen quality and functionality in healthy men consuming a Western-style diet: A randomized controlled trial. Am J Clin Nutr 108: 953-962, 2018.
47. Qi X, Shang M, Chen C, Chen Y, Hua J, Sheng X, Wang X, Xing K, Ni H and Guo Y: Dietary supplementation with linseed oil improves semen quality, reproductive hormone, gene and protein expression related to testosterone synthesis in aging layer breeder roosters. Theriogenology 131: 9-15, 2019.
48. Gianzo M and Subirán N: Regulation of male fertility by the renin-angiotensin system. Int J Mol Sci 21: 7943, 2020.
49. Ma P, Zhang Z, Zhou X, Luo J, Lu H and Wang Y: Characterizing semen abnormality male infertility using non-targeted blood plasma metabolomics. PLoS One 14: e0219179, 2019.
50. Malik IA, Durairajanayagam D and Singh HJ: Leptin and its actions on reproduction in males. Asian J Androl 21: 296-299, 2019.
51. Haron MN, D'Souza UJ, Jaafar H, Zakaria R and Singh HJ: Exogenous leptin administration decreases sperm count and increases the fraction of abnormal sperm in adult rats. Fertil Steril 93: 322-324, 2010.
52. Barbagallo F, Condorelli RA, Mongioì LM, Cannarella R, Cimino L, Magagnini MC, Crafa A, La Vignera S and Calogero AE: Molecular mechanisms underlying the relationship between obesity and male infertility. Metabolites 11: 840, 2021.
53. Leisegang K, Sengupta P, Agarwal A and Henkel R: Obesity and male infertility: Mechanisms and management. Andrologia 53: e13617, 2021.
54. Wang H, Lv Y, Hu K, Feng T, Jin Y, Wang Y, Huang Y and Chen B: Seminal plasma leptin and spermatozoon apoptosis in patients with varicocele and leucocytospermia. Andrologia 47: 655-661, 2015.
55. Martin LJ: Implications of adiponectin in linking metabolism to testicular function. Endocrine 46: 16-28, 2014.
56. Choubey M, Ranjan A, Bora PS, Baltazar F, Martin LJ and Krishna A: Role of adiponectin as a modulator of testicular function during aging in mice. Biochim Biophys Acta Mol Basis Dis 1865: 413-427, 2019.
57. Zhang HZ, Hao SL and Yang WX: How does retinoic acid (RA) signaling pathway regulate spermatogenesis? Histol Histopathol 37: 1053-1064, 2022.
58. Hernández-Silva G, Caballero-Campo P and Chirinos M: Sperm mRNAs as potential markers of male fertility. Reprod Biol 22: 100636, 2022.
59. Corral-Vazquez C, Salas-Huetos A, Blanco J, Vidal F, Sarrate Z and Anton E: Sperm microRNA pairs: New perspectives in the search for male fertility biomarkers. Fertil Steril 112: 831-841, 2019.
60. Courey-Ghaouzi AD, Kleberg L and Sundling C: Alternative B cell differentiation during infection and inflammation. Front Immunol 13: 908034, 2022.
61. Tohyama Y, Takano T and Yamamura H: B cell responses to oxidative stress. Curr Pharm Des 10: 835-839, 2004.
62. Yu W, Li C, Zhang D, Li Z, Xia P, Liu X, Cai X, Yang P, Ling J, Zhang J, *et al*: Advances in T cells based on inflammation in metabolic diseases. Cells 11: 3554, 2022.
63. Seshadri S, Flanagan B, Vince G and Lewis-Jones DJ: Detection of subpopulations of leucocytes in different subgroups of semen sample qualities. Andrologia 44 (Suppl 1): S354-S361, 2012.
64. Chu DS and Shakes DC: Spermatogenesis. Adv Exp Med Biol 757: 171-203, 2013.
65. Coutton C, Vargas AS, Amiri-Yekta A, Kherraf ZE, Ben Mustapha SF, Le Tanno P, Wambergue-Legrand C, Karaouzène T, Martinez G, Crouzy S, *et al*: Mutations in CFAP43 and CFAP44 cause male infertility and flagellum defects in Trypanosoma and human. Nat Commun 9: 686, 2018.
66. Ben Khelifa M, Coutton C, Zouari R, Karaouzène T, Rendu J, Bidart M, Yassine S, Pierre V, Delaroche J, Hennebicq S, *et al*: Mutations in DNAH1, which encodes an inner arm heavy chain dynein, lead to male infertility from multiple morphological abnormalities of the sperm flagella. Am J Hum Genet 94: 95-104, 2014.